Direct Molecular Dynamics Simulation of Branch Point Motion in Asymmetric Star Polymer Melts

Qiang Zhou and Ronald G. Larson*

Department of Mechanical Engineering, University of Michigan, Ann Arbor, Michigan 48109-2136

Received January 10, 2007; Revised Manuscript Received February 23, 2007

ABSTRACT: The conjecture that branched polymers relax hierarchically in entangled melts is herein verified using microscopic molecular dynamics (MD) simulations of symmetric and asymmetric star polymers made possible by an efficient equilibration method. At time scales less than the short-arm relaxation time, the branch point remains anchored within a length scale of a tube diameter. Once the short arm relaxes, the branch point takes a random hop along the confining tube where the distinct "hop" can be visualized directly by simulation. At time scales much larger than the short-arm relaxation time, the branch point becomes mobile enough to allow the backbone to reptate. Coarse-grained simulations of a one-dimensional Rouse chain diffusing along a three-dimensional random walk with the short arm replaced by a large friction bead at the branch point capture the dynamics of the asymmetric star polymer at time scales larger than the short-arm relaxation time. Our simulations also suggest that branches that are only one or two entanglements long slow the motion of the branch point more than expected by a naive application of the hierarchical model because on the time scale for relaxation of such short arms the entanglement spacing is effectively smaller than at longer times, making the short arm effectively more entangled than expected.

I. Introduction

A long-chain polymer in a melt relaxes its configuration through curvilinear diffusion, called reptation, along a tubelike region as the result of the collective topological constraints imposed by neighboring polymers.[1,2] Using this "tube" model, Doi[3] and Milner and MeLeish[4] successfully predicted that the zero-shear viscosity of long-chain polymer melts follows roughly a 3.4 power law scaling with the molecular weight, consistent with experimental results.

However, a symmetric star polymer, in which a single branch point joins three or more arms of equal molecular weight, cannot reptate. The motion of the branch point is constrained by the entanglements of the star arms with neighboring star polymers. Thus, on short time scales, the branch point is highly localized to a region of roughly one tube diameter. Instead of reptating, a star polymer relaxes its configuration through arm retraction; that is, in a mean-field picture, the tip of a star arm occasionally retracts diffusively along its tube, all the way to the branch point, and then diffuses out toward a new configuration that is uncorrelated with the previous one, thereby relaxing its configuration. This mechanism of arm retraction has been incorporated into a quantitative theory predicting the relaxation of monodisperse symmetric star polymer melts by Milner and McLeish.[5]

The dynamics of reptation and retraction have been cornerstones of the recent development of "analytical rheology", which is an effort to find the relationship between the molecular weight and long-chain branching distributions of a polymer melt and its linear rheological properties. One such effort yielded a so-called hierarchical model,[6−13] which has successfully predicted the linear rheology of branched polymers of complicated structures, such as "H" and "comb" polymers, and blends of these, and a related model even allows predictions for polymers with branches on branches.[14] The key assumption underlying these theories is the "hierarchical" relaxation conjecture,[15] which allows one to break down the relaxation of a branched polymer into a sequence of simple processes of reptation and retraction. A comb polymer, for example, has multiple arms of different lengths growing from different branch points distributed along a single linear backbone. According to the hierarchical model, all the dangling arms of the comb polymer initially retract similarly as do the arms of a symmetric star polymer until they retract completely to the branch points, after which the arms on the comb can be conceptually treated as "frictional beads" located at the branch points. The additional drag contributed to the backbone by these frictional beads is controlled by the longest relaxation time of the dangling arms. Once all the arms "collapse" to the backbone, the backbone undergoes reptation motion just as a linear polymer does, except that the comb backbone reptation is slowed down by the "fat" beads located at the branch points. A general framework that allows this hierarchical model to be applied to commercial polymer melts was also proposed by Larson.[7]

What is still missing, however, is microscopic evidence of this hierarchical relaxation. Testing this "hierarchical conjecture" is in an urgent need to justify and further enhance the capability of models that include branch-point motion, such as the hierarchical model. To this end, this work aims to verify the hierarchical relaxation conjecture using MD simulations of asymmetric three-arm star polymers, the simplest branched polymers that capture the essence of hierarchical relaxation. In the asymmetric stars considered here, there is only one branch point, which is located at the center of a linear "backbone", with a single short dangling arm attached to the linear polymer at the branch point. The hierarchical relaxation conjecture for this polymer applies as follows. Starting from an equilibrium configuration, at time scales less than the short-arm relaxation time, the branch point remains anchored to a region comparable to a tube diameter, while the short arm initially relaxes as would a branch on a symmetric star polymer. However, at a time comparable to the short-arm relaxation time, the short arm has retracted back to the branch point, and this allows the branch point to take a random hop along the confining tube. At time scales much larger than the short-arm relaxation time, the branch

10.1021/ma070072b CCC: $37.00
Published on Web 03/29/2007

point has hopped many times, and the backbone is able to assume reptation motion. The dynamics of the asymmetric star at these long time scales can be represented simply by a linear backbone except with the short arm replaced by a large frictional bead.

In this paper, we will examine each of the steps involved in the hierarchical relaxation conjecture. The rest of the paper is organized as follows: In section II, we will briefly describe the polymer model and simulation method we use in this work, followed in section III by an equilibration method we developed for star polymer melts. After that, in section IV we will discuss short-arm relaxation and branch point motion. In section V, we demonstrate the feasibility of capturing asymmetric star dynamics using a coarse-grained linear polymer model that replaces the short arm with a frictional bead located at the branch point. We will then summarize in section VI.

II. Polymer Model and Simulation Method

In this work, polymers are represented as "pearl necklace" chains of beads connected by short springs, as in the model of Kremer and Grest.[16] Excluded volume interactions are included through a repulsive Lennard-Jones potential: $U_{LJ}(r) = 4\epsilon\{(\sigma/r)^{12} - (\sigma/r)^6 + {}^1/_4\}$ where the cutoff distance $r_c = 2^{1/6}\sigma$ is chosen so that only the repulsive part of the Lennard-Jones potential is used. σ and $\tau_0 = (m\sigma^2/\epsilon)^{1/2}$ set the length and time scales, respectively, where m is the bead mass and $\epsilon = k_BT$.

A finitely extensible nonlinear elastic (FENE) potential is used here for the spring: $U_{FENE}(r) = -0.5kR_0^2 \ln(1 - (r/R_0)^2)$. The spring is made short and stiff enough so that there is not enough room between connected beads for another bead to pass between them. Thus, chain crossing is disallowed. We take the spring constant to be $k = 30\epsilon/\sigma^2$ and the maximum length of the spring to be $R_0 = 1.5\sigma$.[16]

In addition, a three-bead bending potential is applied:[17] $U_{bend}(r) = k_\theta(1 - \cos\theta)$, where k_θ is the bending stiffness, and $\cos\theta_i = (\hat{\mathbf{r}}_i - \hat{\mathbf{r}}_{i-1})\cdot(\hat{\mathbf{r}}_{i+1} - \hat{\mathbf{r}}_i)$, with $(\hat{\mathbf{r}}_i - \hat{\mathbf{r}}_{i-1})$ the unit vector pointing from bead $i-1$ to bead i. In this work, we use $k_\theta = 2\epsilon$, which leads to a *semiflexible* polymer with a packing length 0.36σ and a characteristic ratio (proportional to chain stiffness) of $C_\infty = 3.4$, while a standard *flexible* polymer, $k_\theta = 0$, has a packing length 0.68σ and $C_\infty = 1.75$. The packing length is defined as $p = (N-1)/(\rho\langle R^2\rangle)$, where $\langle R^2\rangle$ is the average end-to-end extension. Primitive path analyses yield values of $N_e^p = 65$ and 23 for the number of beads per entanglement for the above *flexible* and *semiflexible* polymer melts, respectively.[18] The use of a *semiflexible* polymer chain therefore allows us to explore more densely entangled polymer melts than is possible with *flexible* ones at the same computational expense.

In our MD simulation, we integrate an equation of motion, namely, $\dot{\mathbf{r}}_i = -\nabla U - \Gamma\dot{\mathbf{r}}_i + W_i(t)$, where $\mathbf{r}_i$ is the position vector for bead i, and the potential U is comprised of the pairwise Lennard-Jones potential, the FENE potential, and the three-body bending potential given above. The segment number density is here set at $\rho = 0.85\sigma^{-3}$. The average monomer length is $\langle l^2\rangle^{1/2} = 0.97\sigma$ and the statistical segment length $b = 1.83\sigma$ where $b \equiv \sqrt{\langle R^2\rangle/N}$. We performed constant NVT simulations in a periodic cubic simulation box coupled with a thermostat through a random force term, $\mathbf{W}_i(t)$, and a dissipation term, $\Gamma\dot{\mathbf{r}}_i$. $\mathbf{W}_i$ is a Gaussian white noise, which is related to the friction coefficient, Γ, by $\langle \mathbf{W}_i(t)\cdot\mathbf{W}_j(t')\rangle = \delta_{ij}\delta(t-t')6k_BT\Gamma$. The temperature is kept at around $T = \epsilon/k_B$ during the simulations, and $\Gamma = 0.5m/\tau_0$. The velocity-Verlet method is used in the integration with a time step size of $\Delta t = 0.01\tau_0$.

III. Equilibration of Star Polymer Melts

The equilibration of asymmetric star polymer melts is a more challenging problem than is the equilibration of linear polymer melts, the latter of which was first successfully accomplished by Auhl et al.[17] Ideally, the best way to generate an equilibrated melt of star polymers is to start from an arbitrary initial configuration and continue an MD simulation out to several times the longest relaxation time of the star. This method is applicable to melts of very small asymmetric stars, i.e., asymmetric stars with a backbone length of only a couple of entanglements and a short arm length of less than an entanglement. However, these small star polymer melts cannot capture the entangled dynamics that we are interested in. With current computer speed, we can only afford with this method to equilibrate linear polymers of up to five entanglements each. It is very hard to go much beyond this limit since the longest relaxation time of a linear polymer scales with molecular weight to the 3.4 power. It is even worse for a star polymer for which the longest relaxation time is exponentially dependent on arm length. Therefore, a much more efficient equilibration method is needed to study the dynamics of well-entangled asymmetric star polymer melts.

In this section, we demonstrate such a method, which is an extension of the slow "push-off" method developed by Auhl et al.[17] The key idea is to generate initial configurations that are as close as possible to equilibrated ones at large length scales so that MD simulation is only needed to relax the short-length-scale configurations. To the best of our knowledge, this is the first attempt to equilibrate star polymer melts using MD simulations of pearl-necklace chains. This method involves three steps. In the first step, the linear backbones are equilibrated, followed by growing short arms from the linear backbones in the second step. In the final step, the star polymers are equilibrated in a melt.

In the first step, a small system, a box containing 500 chains of 100 beads each, is equilibrated through an MD simulation. Next, we pull all the chains from the simulation box and cut them into halves to construct a database of "building blocks",[19] which are short chains of 50 beads each. We then generate 200 long chains by randomly joining end-to-end these building blocks into chains of 350 beads. Then, we pack these isolated chains into a melt using the slow "push-off" method by Auhl et al.;[17] that is, we first rearrange these chains in the simulation box to maximize homogeneity in the bead number density and then slowly introduce the interchain excluded volume interactions to pack these chains into a melt. Finally, we perform a full MD simulation of these chain for a time of $10^4\tau_0$ to relax the configurations at short length scales.

In the second step, we pull the linear polymer chains equilibrated in the first step out of the simulation box, taking them to be the linear backbones, and graft a short arm to the center of every backbone. To ensure that the short arms have equilibrated configurations, the short arm configuration is copied from a part of another backbone. After the isolated star polymers are generated, we use the same slow push-off method of Auhl et al., in the final step, to pack them into a melt. We carry out an additional MD simulation of these asymmetric stars for a time of $10^4\tau_0$ to relax sub-tube-diameter configurations.

A series of asymmetric star polymer melts with different short arm lengths, $N_a = 5-175$ beads, are generated using the above method. To assess the effectiveness of this equilibration method, we use two measures of equilibration to examine the melt configurations: the internal end-to-end extension of the short arms and backbones and the "contraction factor". The internal

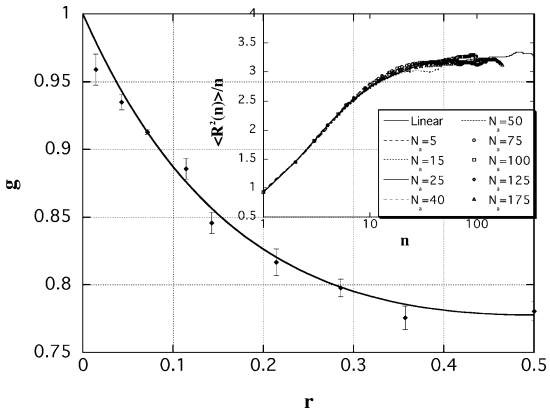

Figure 1. Contraction factor g of asymmetric star polymers as a function of r, the ratio of the arm length to the backbone length, where the solid line is the prediction of the Zimm−Stockmayer theory (eq 2). The inset shows the internal end-to-end separations of the short arms as well as of the linear backbones.

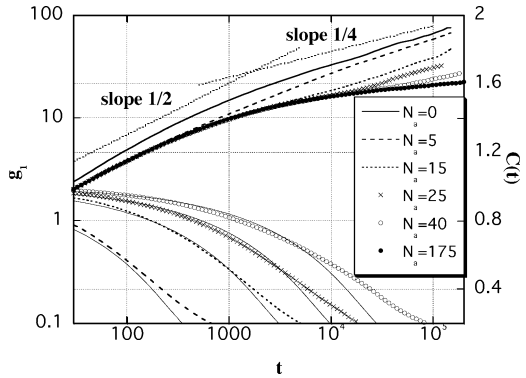

Figure 2. Dielectric relaxation function, $C(t)$ (lower curves), of the short arm of asymmetric star polymers and the mean-square displacements, $g_1(t)$ (upper curves), of the center point of the linear chain, $N_a = 0$, and of the branch points of the asymmetric star polymers, with $N_a = 5-40$, as well as of the branch points of the symmetric star polymer, with $N_a = 175$. The thin lines are fits to $C(t)$ discussed in the text.

end-to-end extension, $\langle R^2(n)\rangle/n$, is an excellent measure of the chain configuration at all length scales. In the inset of Figure 1, we show the internal end-to-end distance of the short arms of different asymmetric star melts as well as of the linear backbones. In an equilibrated melt, the internal end-to-end separation should smoothly and monotonically plateau to a value that is only dependent on the chain stiffness since the star arms and backbones take random walk configurations in melts. As we can see in Figure 1, the end-to-end separations of the short arms all follow the "master curve" of the linear backbones, since they all have the same stiffness. The plateau value agrees well with that of Auhl et al.[17]

In addition to the internal end-to-end extension, the "contraction factor" is another effective measure of the size of the asymmetric star polymer chains. The Zimm−Stockmayer calculation[20,21] provides a theoretical value for this quantity for an equilibrated asymmetric star melt.

The contraction factor is defined as

$$g = \frac{\langle R_g^2\rangle_{\text{branched}}}{\langle R_g^2\rangle_{\text{linear}}} \tag{1}$$

where $\langle R_g^2\rangle_{\text{branched}} = \sum_{i=1}^{N}\langle (r_i - r_m)^2\rangle/N$ is the radius of gyration of an asymmetric star polymer with N the total number of beads in the polymer, and $r_m = \sum_{i=1}^{N} r_i$ the center of mass

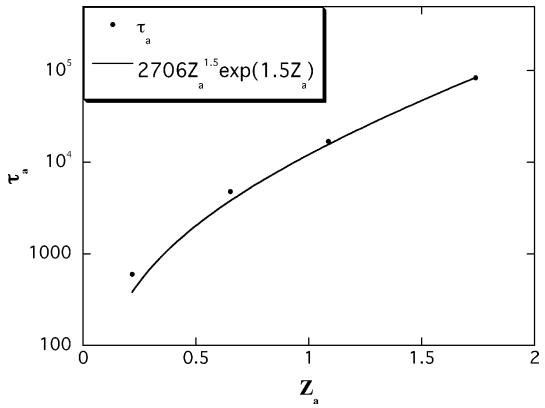

Figure 3. Longest relaxation time, τ_a, of the short arm of the asymmetric star polymer as a function of the short arm length, where $Z_a = N_a/N_e^P$.

Table 1. Relaxation Times of the Short Arms of the Asymmetric Star Polymers[a]

	$N_a = 5$	$N_a = 15$	$N_a = 25$	$N_a = 40$
τ_1	250	2200	7000	20000
τ_1/N^2	10	9.8	11.2	12.5
τ_a	600	4800	17000	84000

[a] Each backbone contains 351 beads including the branch point. τ_1 is obtained by fitting the dielectric relaxation function from the MD simulations by the prediction of the Rouse model (eq 4). τ_a is the characteristic time of the short arm of the asymmetric star.

of the polymer. $\langle R_g^2\rangle_{\text{linear}}$ is the radius of gyration of a linear polymer of the same molecular weight as the star polymer, which can be estimated using the plateau value in the internal end-to-end extension, $\langle R_g^2\rangle_{\text{linear}} \approx 0.542N$.

For an asymmetric star, the Zimm−Stockmayer calculation predicts[21]

$$g^{ZS} = 1 - \frac{24r^2}{(1+4r)^3} \tag{2}$$

where r is the ratio of the short arm molecular weight to the backbone molecular weight. Therefore, $r = 0$ corresponds to a linear polymer while $r = 0.5$ corresponds to a symmetric star. Figure 1 shows that the calculated g from the equilibrated samples is consistent with the Zimm−Stockmayer value. The error bars were obtained by equilibrating three to five different star melts using this equilibration method.

IV. Short Arm Relaxation and Branch Point Motion

Once equilibrated star polymer melts are obtained, we carry out further MD simulations for a time of $5.0 \times 10^5\tau_0$ to explore branch point diffusion behavior. The systems we study here each contain 200 polymers; each polymer has a backbone of 351 beads, including the branch point, and a short arm with length ranging from $N_a = 0$, which are linear chains, up to $N_a = 175$, which are symmetric stars. The backbone has a length of more than 15 entanglements estimated using $N_e^P \approx 23$.

To study the relaxation of the short arms, we compute the dielectric relaxation function, defined as

$$C(t) = \langle \mathbf{P}(t)\cdot\mathbf{P}(t_0)\rangle/\langle |\mathbf{P}(t_0)|^2\rangle \tag{3}$$

where $\mathbf{P}$ is the vector pointing from the branch point to the end bead of the short arm. The lower curves in Figure 2 show the short-arm relaxation functions $C(t)$ of the asymmetric star polymers from the MD simulations.

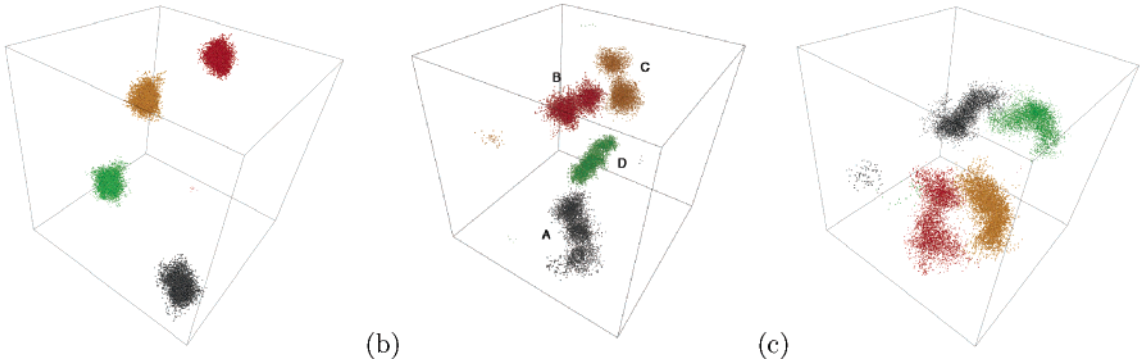

Figure 4. Trajectories of (a) the branch points of four symmetric star polymers, (b) the branch points of four asymmetric star polymers with $N_a = 25$, and (c) the center beads of four linear polymers over a time of $1.35 \times 10^5 \tau_0$.

In the case of unentangled chains, for both the free chains and the chains with one tethered end, the Rouse model predicts the following dielectric relaxation function:[1]

$$C(t) = \sum_{\text{odd } p}^{N} \frac{8}{\pi^2 p^2} \exp(-p^2 t/\tau_1) \tag{4}$$

where the characteristic time τ_1 is the Rouse time for the free chains. For chains with one tethered end, τ_1 is 4 times the Rouse time of a free chain of the same length.

The thin solid lines in Figure 2 are fits to $C(t)$ using eq 4. The characteristic times, τ_1, from these fits are given in Table 1. For both the free chains and the tethered chains, $\tau_1 \propto 1/N^2$, if the chains are unentangled. This is the case for chains with very short arms, $N_a = 5$ and $N_a = 15$. However, τ_1 shows a slightly stronger dependence on chain length than a quadratic power as τ_1/N^2 increases for longer arm lengths, as shown in Table 1, indicating that the entanglement effect kicks in when the short arm length reaches around 15−25. This is consistent with the finding of Zhou and Larson,[22] who showed that the entanglement molecular weight is in the range 14−27 depending on how the entanglement spacing N_e is estimated. The entanglement spacing estimated from the time of transition of the monomer mean-square displacements from $g_1(t) \propto t^{1/2}$ to $g_1(t) \propto t^{1/4}$ is $N_e'' \approx 14$; the entanglement molecular weight estimated from the transition from $g_1(t) \propto t^{1/4}$ to $g_1(t) \propto t^{1/2}$ is $N_e'' \approx 27$ while that estimated from calculation of "primitive path" is $N_e^p \approx 23$ (see ref 22). The deviation of $C(t)$ from that predicted by the Rouse theory for unentangled polymers shows up in the terminal relaxation of the short arms, even for the asymmetric star polymers with $N_a = 5$ (see Figure 2). As the arm length increases, the deviation becomes more prominent.

Also shown in Figure 2 are the mean-square displacements, defined as $g_1(t) = ((\mathbf{r}_b(t) - \mathbf{r}_b(0))^2)$, where $\mathbf{r}_b$ is the branch point position of the star polymer and the center point of the linear polymer. To obtain a smoother function, for the linear chain, the average is taken over the center six beads; for the star polymers, the average is taken over the branch point and its three nearest neighbors. The tube theory predicts a transition at τ_e from unentangled sub-Fickian diffusion, $g_1(t) \propto t^{1/2}$, to entangled sub-Fickian diffusion, $g_1(t) \propto t^{1/4}$. τ_e is the time it takes for the chain to feel the existence of the confining tube. This transition from $g_1(t) \propto t^{1/2}$ to $g_1(t) \propto t^{1/4}$ is captured by simulation of the linear polymers, $N_a = 0$, as shown in Figure 2. The 1/4 power scaling law beginning at time $t \approx t_e$ is generally regarded as evidence of reptation motion in a confining tube.[23]

The branch point of the symmetric star polymer starts with sub-Fickian diffusion, $g_1 \propto t^{1/2}$, but soon localizes once the molecule samples the confining tube at around $g_1 \approx 18$. For each asymmetric star polymer, the branch points initially follows the $g_1(t)$ curve of the symmetric star until, at a time τ_a that depends on the length of the short arm, takes off from this symmetric star curve at the point at which the short arm has relaxed to $C(t) \approx 0.2$. We take τ_a to be the characteristic time of the short arm, and their values are also listed in Table 1. These times are significantly larger than those obtained by fits to the Rouse model, even for the shortest arm that has only five beads and would normally be considered "unentangled". The arm relaxation time τ_a is roughly exponentially dependent on the length of the short arm, as shown in Figure 3. Once the short arm relaxes, the branch point of the asymmetric star polymer follows a $g_1(t) \propto t^{1/4}$ diffusion, shown in Figure 2. That is, the backbone begins to reptate as is assumed by the hierarchical conjecture.

To monitor branch point motion, we show in Figure 4 the trajectories of the branch points of four symmetric star polymers in Figure 4a, four asymmetric star polymers with a short arm of length $N_a = 25$ in Figure 4b, and the center points of four linear polymers in Figure 4c, over a time of $1.35 \times 10^5 \tau_0$. Over this time span, the branch points of the symmetric star polymers are localized in a roughly spheroidal region of diameter comparable to a tube diameter (see Figure 4a). The center points of linear polymers, on the other hand, traverse roughly homogeneously along a portion of the confining tube (see Figure 4c). The branch points of the asymmetric stars, however, show two or more distinct clusters of positions suggestive of a hopping process along a tube. At short time scales, $t < \tau_a$, these branch points are localized just as are the branch points of the symmetric stars. At large time scales, $t > \tau_a$, they diffuse by "hopping" along a portion of a tube, which, if the clusters could be "blurred" together, would create trajectories that look like those of the center points of the linear chains. In Figure 5, we plot the absolute displacement, $|\mathbf{r}_b(t) - \mathbf{r}_b(0)|$, of the branch points of the asymmetric stars shown in Figure 4b. Branch points A and D have three plateaus in the absolute displacement, corresponding to the three blobs in Figure 4b; branch points B and C have only two plateaus, corresponding to the two blobs in Figure 4b. In addition, branch point D shows the random character of the hops; this branch takes a large hop forward along the confining tube and then a small hop backward. The trajectory shown in Figure 6 is from a branch point that happens to hop multiple times in the same direction along the confining tube, over a larger time span of $3.6 \times 10^5 \tau_0$. The absolute displacement for this branch point is shown in Figure 7. Although this is a rare trajectory, since the branch point's random hops happen to take it monotonically in a single direction along the tube, it is very illustrative of both the hopping

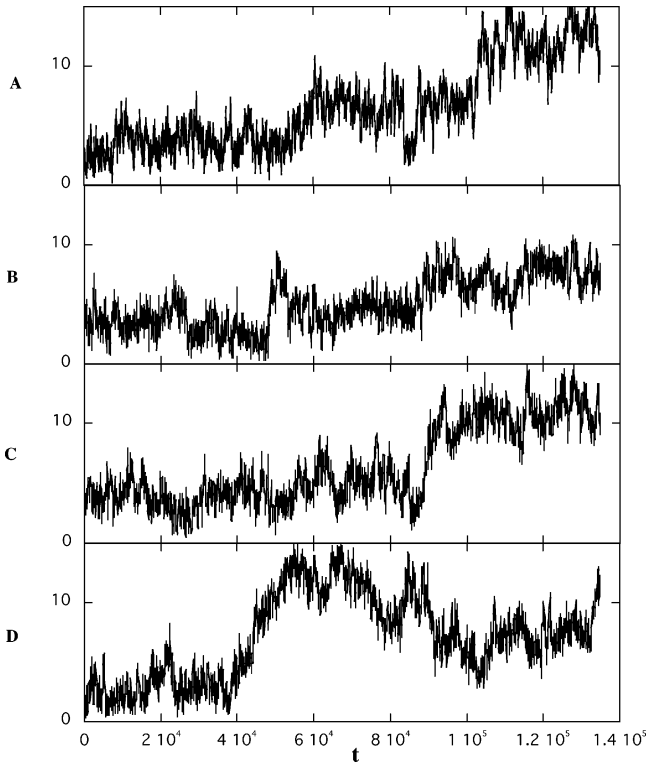

Figure 5. Absolute displacement, $|\mathbf{r}_b(t) - \mathbf{r}_b(0)|$, of the branch points of the four asymmetric star polymers shown in Figure 4b.

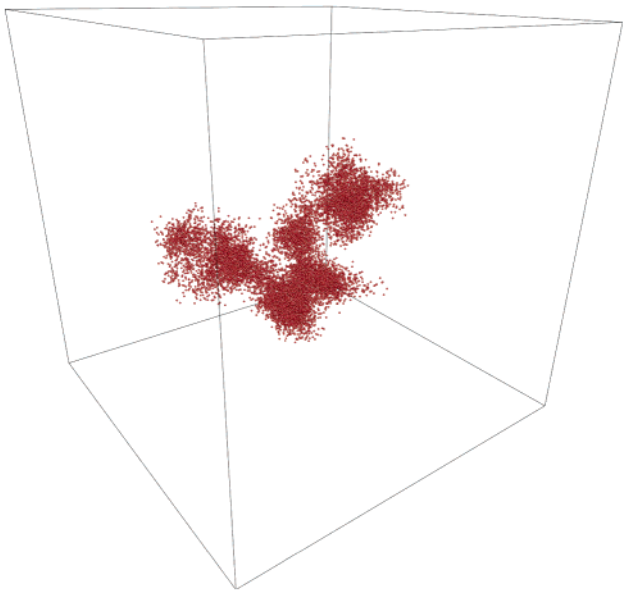

Figure 6. Trajectory of one branch point of an asymmetric star polymer with $N_a = 25$.

process and the tube confinement.

V. Coarse-Graining the Dynamics of Short Arms

The hierarchical conjecture, applied to asymmetric stars, is that at time scales much larger than the longest relaxation time of the short arms the backbone diffuses by reptation with the branch point replaced by a bead whose friction is set by the relaxation time of the short arm and is therefore larger than that of the other beads on the backbone. It is the aim of this section to test the validity of this approach.

According to the tube model, the dynamics of an entangled linear chain can be captured by a Rouse chain undergoing

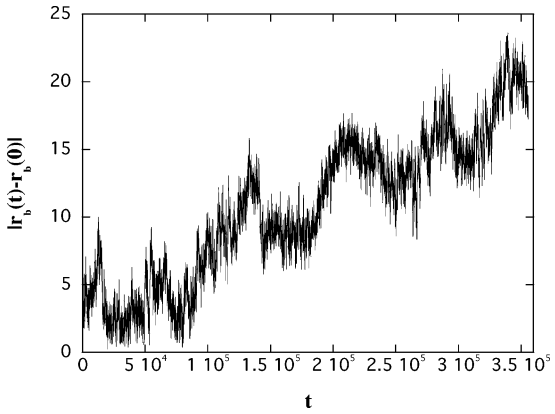

Figure 7. Absolute displacement, $|\mathbf{r}_b(t) - \mathbf{r}_b(0)|$, of the branch point shown in Figure 6.

curvilinear diffusion along a three-dimensional random walk representing the centerline of the confining tube. Here, we represent the linear polymer by a one-dimensional bead−spring Rouse chain. Both ends of the Rouse chain are subject to a constant force to represent the effect of the confinement.[1] The governing equations are listed below:

for internal beads ($i = 1, ..., N_s - 1$):

$$\frac{dR_i}{dt} = -\frac{K_s}{\xi}(2R_i - R_{i+1} - R_{i-1}) + f_i \tag{5}$$

for end beads:

$$\frac{dR_0}{dt} = -\frac{K_s}{\xi}(R_0 - R_1) + f_0 - \frac{3k_BT}{a} \tag{6}$$

$$\frac{dR_{N_s}}{dt} = -\frac{K_s}{\xi}(R_{N_s} - R_{N_s} - 1) + f_{N_s} + \frac{3k_BT}{a} \tag{7}$$

where R_i is the one-dimensional coordinate of bead i, K_s is the spring constant, ξ is the drag coefficient, f_i is the Brownian force term, a is the tube diameter, N_s is the number of springs, $\langle f_i(t)\rangle = 0$, and $\langle f_i(t)f_j(t')\rangle = 6k_BT\delta_{ij}\delta(t - t')$.

The linear pearl-necklace chain in our MD simulations has a Kuhn step length $l_K = 3.34$, the number of Kuhn steps in the chain is $N_K = 102$, and the tube diameter $a = (N_e^P N_K/N l_K)^{1/2} = 8.65$. Also, $K_s = 3k_BT/(N_{K,s}l_K^2)$, where $N_{K,s} = N_K/N_s$. The diffusion function $g_1(t)$ of linear pearl-necklace chain in the unentangled sub-Fickian diffusion regime follows $g_1(t) = 2b^2(Wt)^{1/2} \approx 0.4475\sqrt{t}$,[22] which leads to an average drag coefficient per bead in the pearl-necklace chain of $\xi_0 = 222.83$; thus $\xi = N_{K,s}\xi_0$. All the parameters used in our one-dimensional Rouse model are, therefore, derived directly from the fine-grained pearl-necklace model except for N_s, which sets the desired level of coarse-graining. All beads in the Rouse chain have only a one-dimensional curvilinear coordinate along the confining tube. We represent this tube by a three-dimensional random walk with a step size a, which is the tube diameter. Each node of this three-dimensional random walk has three-dimensional coordinates as well as a one-dimensional curvilinear coordinate, where the linear coordinate is that of the one-dimensional Rouse chain.

The simulation starts with a one-dimensional Rouse chain and its corresponding confining tube which is a three-dimensional random walk. The tube is only long enough to "confine" the Rouse chain. We use a simple renewal and destruction procedure to update the tube configuration. Once

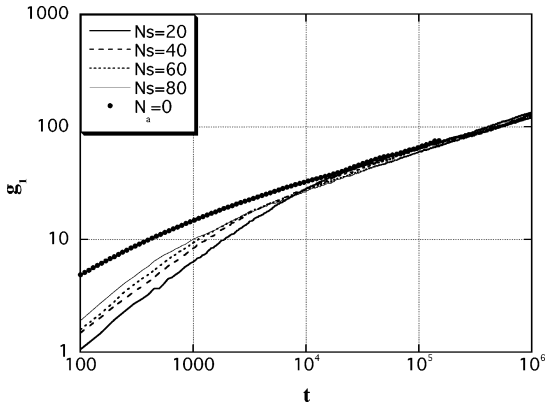

Figure 8. Mean-square displacement of the center beads of a linear chain from MD simulations and from simulations of a one-dimensional Rouse chain with various numbers of springs.

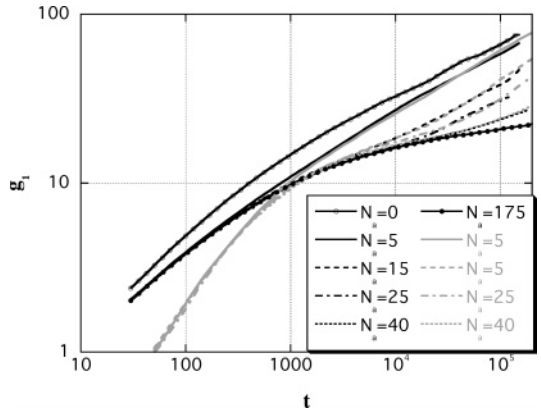

Figure 9. Mean-square displacement of the bead four beads away from the branch point of asymmetric star polymers from MD simulations and of the corresponding bead in the simulations of the one-dimensional Rouse chains. The black lines are from the MD simulations while the gray lines are from the simulations of the one-dimensional Rouse chains.

part of the Rouse chain diffuses out of the end of the tube, more random-walk steps are added to this end to keep the Rouse chain "confined" by the tube at all times. Similarly, all tube segments that are not occupied by the Rouse chain are destroyed as soon as they are vacated. During the simulation, the confining tube experiences many renewal and deconstruction events at both ends, as the Rouse chain diffuses along the tube. Since the tube and the Rouse chain share the same one-dimensional path, it is straightforward to map the Rouse bead position to its corresponding three-dimensional coordinates. We do not incorporate constraint release into this model since this relaxation mechanism is not important at time scales less than the Rouse time, which is the largest time scale that our MD simulation can reach.

Equation 5 is numerically integrated using the Euler forward scheme with a time step size $\Delta t = 0.1\tau_0$. We carried out an initial simulation with an ensemble of 100 chains to a time long enough to relax the initial configuration. Then we run simulations of these Rouse chains to a time of $10^7\tau_0$ to study the diffusion behavior. Figure 8 compares the center bead mean-square displacements for linear polymers from the MD simulations of the pearl-necklace chain and for the corresponding one-dimensional Rouse chain with various numbers of springs. At time scales smaller than equilibration time, $\tau_e = 1800 \pm 100\tau_0$, we do not expect the Rouse chain to capture the correct dynamics since these small-scale dynamics, which describe the process by which the three-dimensional pearl-necklace chain "discovers" that it is in a one-dimensional tube, are coarse-grained away in the one-dimensional Rouse chain. At time scales larger than τ_e, however, we see agreement between the pearl necklace results and those of the Rouse model. Note that only $N_s = 20$ Rouse springs are needed to reproduce the dynamics of the pearl necklace chain at time scales larger than τ_e and that our Rouse chain simulations are free of any adjustable parameters, all parameters having been obtained from the original MD simulations.

For asymmetric stars, the effective diffusion coefficient of the branch point is estimated as[6]

$$D = k_B T/\xi = p^2 a^2/2\tau_a \tag{8}$$

where τ_a is the longest relaxation time of the short arm. We estimate this time, listed in Table 1, as the time at which g_1 deviates from that for symmetric stars. p is an order one constant, which is usually determined in hierarchical models through fitting of the theory to experimental data. In this way, p^2 has been found to be 1/12 for well-entangled "H" and "comb" polymers.[6,13] For asymmetric star polymers, however, Frischknecht[24] found that the value of p^2 depends on the length of the short arm, ranging from 1/60 to 1/4 from short to long ones, and it is usually much smaller than 1/12 when the short arms are only a few entanglements long.

To coarse-grain the behavior of asymmetric star polymers, we use the same one-dimensional Rouse chain of 80 springs that we used for linear chains but replace the center bead drag coefficient with the one calculated from eq 8 for the branch point. This large bead is extremely sluggish and cannot represent the small-scale motions of the branch point at time scales less than τ_a. It is therefore more reasonable to track the motion of the bead next to the branch point bead, rather than the motion of the branch-point bead itself. Figure 9 shows $g_1(t)$ of the bead next to the "fat" bead from the one-dimensional Rouse simulations and the corresponding bead, which is four beads away from the branch point bead, on the backbone of the asymmetric star polymers in the MD simulations. We note that the bead close to the branch point in the MD simulation has nearly identical diffusion behavior to that of the branch point. At time scales larger than τ_e, each simulation of the Rouse chain shows excellent agreement with the MD simulation of the corresponding asymmetric star polymer, if p^2 is taken to be 1/60, 1/50, 1/42, and 1/32 for $N_a = 5$, 15, 25, and 40, respectively, which are consistent with the values used by Frischknecht.[24] Thus, our simulations seem to be consistent with experimental data on asymmetric stars, which can also be modeled by the hierarchical model, if the value of p^2 is reduced for the shorter arms.

VI. Discussion and Summary

Using direct MD simulations, our paper validates, for the first time, the "hierarchical hypothesis" that the effect of a branch on polymer diffusion at time scales greater than τ_e can be modeled by replacing the branch with a frictional bead with friction coefficient inversely proportional to the relaxation time of the branch. To do so, an efficient equilibration method is proposed in this paper to prepare melts of asymmetric star-branched polymers modeled using pearl-necklace chains.

At early stages of the relaxation process, the short arm of the asymmetric star polymer relaxes while the branch point is localized in a manner similar to that of a symmetric star. Once the short arm relaxes, the branch point takes discrete random hops along the confining tube. Our molecular dynamics simula-

tions capture these microscopic hopping events for an asymmetric stars with a dangling arm as short as about one entanglement long. The random hopping events in a confining tube lead at long times to an effective reptation of the whole backbone, as is conjectured by the hierarchical model.

At time scales larger than the longest relaxation time of the short arm, i.e., longer than the characteristic hopping time, the dynamics of the asymmetric star polymers can be effectively represented by the linear backbone but with the short arm replaced by a "fat" frictional bead located at the branch point. The effective drag coeficient of this "fat" bead is determined by the relaxation time of the short arm. This approach of coarse-graining is validated by a coarse-grained simulation model, namely a one-dimensional Rouse chain diffusing along a three-dimensional random walk representing the tube.

Our coarse-grained simulation shows, in agreement with inferences from experimental data, that in an asymmetric star polymer with a short dangling arm having only one or two entanglements, the branch point has a much higher effective drag than the hierarchical model predicts, using the "conventional" value of the prefactor $p^2 = 1/12$. Part of the reason seems to be that the apparent tube diameter is time dependent over the range of times extending from the equilibration time τ_e to the Rouse time τ_R.[22] Thus, for short arms that relax at time scales close to τ_e, the effective entanglement spacing is about $N_e' = 14$, significantly smaller than the entanglement spacing at longer times near the Rouse times, where $N_e'' \approx 27$ is close to N_e^P, the latter of which is the same as the value of N_e estimated from the plateau modulus.[25] Moreover, the short arm relaxation time also significantly differs from that for an unentangled Rouse chain when the arm is as short as 15 beads long (see Figure 2). This early occurrence of the entanglement effect at times near τ_e, we believe, is responsible for the larger than expected effective drag of a short arm. Thus, an arm whose length is less than a single entanglement, as measured using the long-time entanglement spacing, N_e^P, can be longer than one entanglement if we use the entanglement spacing N_e', which is more appropriate measure at time scales near τ_e.

Acknowledgment. This work was supported by the NSF under Grant DMR 0305437 and supported by the National Computational Science Alliance under PHY040025N, utilizing the IBM P690 Supercluster. Any opinions, findings, and conclusions or recommendations expressed in this material are those of the authors and do not necessarily reflect the views of the National Science Foundation (NSF). Helpful discussions with Dr. Alexei Likhtman and Dr. Sachin Shanbhag are gratefully acknowledged.

References and Notes

(1) Doi, M.; Edwards, S. F. *The Theory of Polymer Dynamics*; Oxford University Press: New York, 1986.
(2) de Gennes, P. G. Reptation of a polymer chain in the presence of fixed obstacles. *J. Chem. Phys.* **1971**, *55*, 572−579.
(3) Doi, M. Explanation for the 3.4-power law for viscosity of polymeric liquids on the basis of the tube model. *J. Polym. Sci., Part B: Polym. Phys.* **1983**, *21*, 667−684.
(4) Milner, S. T.; McLeish, T. C. B. Reptation and contour-length fluctuations in melts of linear polymers. *Phys. Rev. Lett.* **1998**, *81*, 725−728.
(5) Milner, S. T.; McLeish, T. C. B. Parameter-free theory for stress relaxation in star polymer melts. *Macromolecules* **1997**, *30*, 2159−2166.
(6) McLeish, T. C. B.; Allgaier, J.; Bick, D. K.; Bishko, G.; Biswas, P.; Blackwell, R.; Blottiere, B.; Clarke, N.; Gibbs, B.; Groves, D. J.; Hakiki, A.; Heenan, R. K.; Johnson, J. M.; Kant, R.; Read, D. J.; Young, R. N. Dynamics of entangled H-polymers: Theory, rheology, and neutron-scattering. *Macromolecules* **1999**, *32*, 6734−6758.
(7) Larson, R. G. Combinatorial rheology of branched polymer melts. *Macromolecules* **2001**, *34*, 4556−4571.
(8) Park, S. J.; Larson, R. G. Dilution exponent in the dynamic dilution theory for polymer melts. *J. Rheol.* **2003**, *47*, 199−211.
(9) Park, S. J.; Larson, R. G. Tube dilation and reptation in binary blends of monodisperse linear polymers. *Macromolecules* **2004**, *37*, 597−604.
(10) Park, S. J.; Larson, R. G. Modeling the linear viscoelastic properties of metallocene-catalyzed high density polyethylenes with long-chain branching. *J. Rheol.* **2005**, *49*, 523−536.
(11) Park, S. J.; Shanbhag, S.; Larson, R. G. A hierarchical algorithm for predicting the linear viscoelastic properties of polymer melts with long-chain branching. *Rheol. Acta* **2005**, *44*, 319−330.
(12) Park, S. J.; Larson, R. G. Long-chain dynamics in binary blends of monodisperse linear polymers. *J. Rheol.* **2006**, *50*, 21−39.
(13) Inkson, N. J.; Graham, R. S.; McLeish, T. C. B.; Groves, D. J.; Fernyhough, C. M. Viscoelasticity of monodisperse comb polymer melts. *Macromolecules* **2006**, *39*, 4217−4227.
(14) Das, C.; Inkson, N. J.; Read, D. J.; Kelmanson, M. A.; McLeish, T. C. B. Computational linear rheology of general branch-on-branch polymers. *J. Rheol.* **2006**, *50*, 207−235.
(15) Mcleish, T. C. B. Hierarchical-relaxation in tube models of branched polymers. *Europhys. Lett.* **1988**, *6*, 511−516.
(16) Kremer, K.; Grest, G. S. Dynamics of entangled linear polymer melts - a molecular-dynamics simulation. *J. Chem. Phys.* **1990**, *92*, 5057−5086.
(17) Auhl, R.; Everaers, R.; Grest, G. S.; Kremer, K.; Plimpton, S. J. Equilibration of long chain polymer melts in computer simulations. *J. Chem. Phys.* **2003**, *119*, 12718−12728.
(18) Everaers, R.; Sukumaran, S. K.; Grest, G. S.; Svaneborg, C.; Sivasubramanian, A.; Kremer, K. Rheology and microscopic topology of entangled polymeric liquids. *Science* **2004**, *303*, 823−826.
(19) Zhou, Q.; Larson, R. G. Primitive path identification and statistics in molecular dynamics simulations of entangled polymer melts. *Macromolecules* **2005**, *38*, 5761−5765.
(20) Zimm, B. H.; Stockmayer, W. H. The dimensions of chain molecules containing branches and rings. *J. Chem. Phys.* **1949**, *17*, 1301−1314.
(21) Hadjichristidis, N.; Xenidou, M.; Iatrou, H.; Pitsikalis, M.; Poulos, Y.; Avgeropoulos, A.; Sioula, S.; Paraskeva, S.; Velis, G.; Lohse, D. J.; Schulz, D. N.; Fetters, L. J.; Wright, P. J.; Mendelson, R. A. Garcia-Franco, C. A.; Sun, T.; Ruff, C. J. Well-defined, model long chain branched polyethylene. 1. Synthesis and characterization. *Macromolecules* **2000**, *33*, 2424−2436.
(22) Zhou, Q.; Larson, R. G. Direct calculation of the tube potential confining entangled polymers. *Macromolecules* **2006**, *39*, 6737−6743.
(23) Kremer, K.; Grest, G. S.; Carmesin, I. Crossover from rouse to reptation dynamics—a molecular-dynamics simulation. *Phys. Rev. Lett.* **1988**, *61*, 566−569.
(24) Frischknecht, A. L.; Milner, S. T.; Pryke, A.; Young, R. N.; Hawkins, R.; McLeish, T. C. B. Rheology of three-arm asymmetric star polymer melts. *Macromolecules* **2002**, *35*, 4801−4820.
(25) Putz, M.; Kremer, K.; Grest, G. S. What is the entanglement length in a polymer melt? *Europhys. Lett.* **2000**, *49*, 735−741.

MA070072B